USE OF SUPERCOMPUTERS TO EVALUATE SINGLY AND MULTIPLY SCATTERED ELECTROMAGNETIC FIELDS FROM ROUGH SURFACES

E. BAHAR, fellow member, IEEE, and M. El-SHENAWEE
Department of Electrical Engineering, University of Nebraska, Lincoln.

Abstract **- Full wave expressions for the singly and the doubly scattered electromagnetic fields from one dimensional rough surfaces are computed. The singly scattered like and cross polarized fields are expressed in terms of one dimensional integrals. However the doubly scattered full wave solutions are expressed in terms of two and three dimensional integrals. To compute the like and the cross polarized multiple scattered fields it is necessary to use a supercomputer. The results indicate that double scatter in the backward direction is significant for near normal incidence when the mean square slopes of the highly conducting rough surfaces are larger than unity.**

FORMULATION OF THE PROBLEM

For exp(jωt) time excitations, the full wave solutions for the singly scattered far fields from two dimensional rough surfaces $f(x,y,z)=y-h(x,z)=0$, can be expressed in the matrix form [1] as follows,

$$G^f = \left(\frac{k_o}{2\pi j}\right)^2 \int \frac{D(\bar{n}',\bar{n}^i)}{\bar{n}\cdot\bar{a}_y} e^{j\bar{v}'\cdot\bar{r}'_s} e^{-jk_o\bar{n}'\cdot\bar{r}} U(\bar{r}'_s) \cdot \frac{dn'_y}{n'_x} dn'_z\, dx_s\, dz_s\, G^i \tag{1a}$$

where,

$$\bar{n}' = n'_x\bar{a}_x + n'_y\bar{a}_y + n'_z\bar{a}_z, \quad \bar{n}^i = n^i_x\bar{a}_x + n^i_y\bar{a}_y + n^i_z\bar{a}_z \tag{1b}$$

$$\bar{v}' = k_o(\bar{n}' - \bar{n}^i) \tag{1c}$$

$$\bar{r}'_s = x_s\bar{a}_x + h(x_s, z_s)\bar{a}_y + z_s\bar{a}_z, \quad \bar{r} = x\bar{a}_x + y\bar{a}_y + z\bar{a}_z \tag{1d}$$

$$\bar{n} = \nabla f / |\nabla f| = (-h_{x_s}\bar{a}_x + \bar{a}_y - h_{z_s}\bar{a}_z) / (1 + h^2_{x_s} + h^2_{z_s})^{1/2} \tag{1e}$$

in which $k_o=\omega\sqrt{\mu_o\epsilon_o}$ is the free space wavenumber. The radius vectors from the origin to the rough surface and to the observation point are $\bar{r}'_s$ and $\bar{r}$, respectively, and $\bar{n}'$ and $\bar{n}^i$ are the unit vectors in the directions of the scattered and incident waves, respectively. The elements of the 2×1 matrices G^i and G^f are the vertically and the horizontally polarized field components of the incident and scattered waves, respectively, and the elements of the 2×2 scattering matrices $D(\bar{n}',\bar{n}^i)$ depend on the polarizations and the directions of the incident and scattered waves, the media on both sides of the rough interface, and the unit vector $\bar{n}$ normal to the rough surface [1], [2]. The shadow function $U(\bar{r}'_s)$ is given by

$$U(\bar{r}'_s) = \begin{cases} 1 \text{ if illuminated and visible} \\ 0 \text{ if nonilluminated or nonvisible} \end{cases} \tag{1f}$$

For one dimensional rough surfaces $y=h(x)$, equation (1a) can be readily integrated with respect to z_s and n'_z. Thus (1a) reduces to,

$$G^f = \left(\frac{-k_o}{2\pi}\right) \int\int \frac{D(\bar{n}',\bar{n}^i)}{\bar{n}\cdot\bar{a}_y} e^{j\bar{v}'\cdot\bar{r}_s} e^{-jk_o\bar{n}'\cdot\bar{r}} U(\bar{r}'_s) \frac{dn'_y}{n'_x} dx_s \tag{2a}$$

where,

$$\bar{r}_s = x_s\bar{a}_x + h(x_s)\bar{a}_y, \text{ and} \qquad n'_z = n^i_z \tag{2b}$$

Assuming that $k_o r \gg 1$, we can use the steepest descent method to integrate (2a) with respect to n'_y to obtain the singly scattered far field,

$$G^f_s = -\left(\frac{k_o}{2\pi\rho\,\sin\theta^i_z}\right)^{1/2} e^{-jk_o r} e^{j\pi/4} \int \frac{D(\bar{n}^f,\bar{n}^i)}{\bar{n}\cdot\bar{a}_y} e^{j\bar{v}\cdot\bar{r}_s} U(\bar{r}'_s)\, dx_s \tag{3a}$$

where, $\bar{n}^f$ is the unit vector in the direction of the position vector $\bar{r}$ to the observation point and,

$$\bar{v} = k_o(\bar{n}^f - \bar{n}^i), \qquad r = (x^2 + y^2 + z^2)^{1/2} \tag{3b}$$

$$\rho = (x^2 + y^2)^{1/2}, \quad \sin\theta^i_z = (1 - n^{i\,2}_z)^{1/2} \tag{3c}$$

The singly scattered field G_2 incident upon the surface at $\bar{r}'_{s2}$ can be obtained by using the full wave expression (2). Thus

$$G_2(\bar{r}'_{s2}) = \frac{-k_o}{2\pi} \int\int \frac{D(\bar{n}',\bar{n}^i)}{\bar{n}_1\cdot\bar{a}_y} e^{j\bar{v}'\cdot\bar{r}_{s1}} e^{-jk_o\bar{n}'\cdot\bar{r}'_{s2}} U(\bar{r}'_{s1}) \frac{dn'_y}{n'_x} dx_{s1}\, G^i \tag{4}$$

where $\bar{n}_1$ is a unit vector normal to the rough surface at $\bar{r}'_{s1}$, (see fig.1).

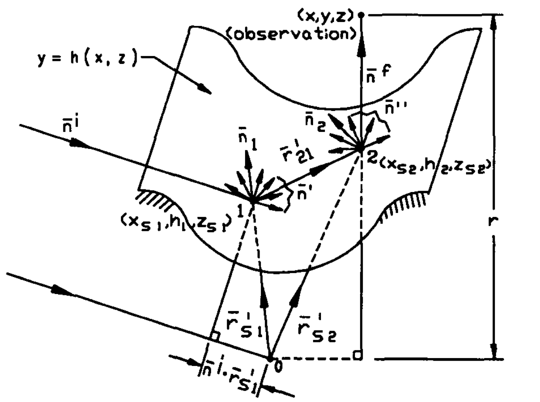

Fig.1 The double scattered electromagnetic waves

The full wave solutions for the doubly scattered electromagnetic

0018-9464/91$01.00 © 1991 IEEE

fields G_d^f, are obtained by substituting $G_2(\bar{r}'_{s2})$ instead of $G^i \exp(-j\bar{n}^i \cdot \bar{r}'_s)$ in (1a). Thus it follows that

$$G_d^f = \left(\frac{k_o}{2\pi j}\right)^2 \int\int\int\int \frac{D(\bar{n}'', \bar{n}')}{\bar{n}_2 \cdot \bar{a}_y} e^{jk_o \bar{n}'' \cdot \bar{r}_{s2}} e^{-jk_o \bar{n}'' \cdot \bar{r}} \cdot U(\bar{r}'_{s2})\ G_2(\bar{r}'_{s2}) \cdot \frac{dn''_y}{n''_x} dn''_z\, dx_{s2}\, dz_{s2} \tag{5}$$

Assuming that $k_o r \gg 1$, the steepest descent method can be used to integrate (5) with respect to n''_y, thus

$$G_d^f = \left(\frac{k_o}{2\pi}\right)^2 \left(\frac{2\pi}{k_o \rho \sin\theta_z^i}\right)^{1/2} e^{j\pi/4} e^{-jk_o r} \int\int \frac{D(\bar{n}^f, \bar{n}')}{\bar{n}_2 \cdot \bar{a}_y} \frac{D(\bar{n}', \bar{n}^i)}{\bar{n}_1 \cdot \bar{a}_y} U(\bar{r}'_{s1})\ U(\bar{r}'_{s2}) \cdot e^{jk_o(\bar{n}^f \cdot \bar{r}_{s2} - \bar{n}^i \cdot \bar{r}_{s1} - \bar{n}' \cdot \bar{r}_{21})} \frac{dn'_y}{n'_x} dx_{s1}\, dx_{s2} \tag{6a}$$

where,

$$\bar{n}^f = n_x^f \bar{a}_x + n_y^f \bar{a}_y + n_z^f \bar{a}_z, \quad n_z^f = n_z^i, \quad \bar{r}_{21} = \bar{r}_{s2} - \bar{r}_{s1} \tag{6b}$$

Assuming that $k_o r_{21} \gg 1$, we can apply the steepest descent approximation to integrate (6) with respect to n'_y. Thus (6) reduces to

$$G_d^f = \left(\frac{k_o}{2\pi}\right) \frac{e^{-jk_o r} e^{j\pi/2}}{(\rho)^{1/2} \sin\theta_z^i} \int\int \frac{D(\bar{n}^f, \bar{n}_{21})}{\bar{n}_2 \cdot \bar{a}_y} \frac{D(\bar{n}_{21}, \bar{n}^i)}{\bar{n}_1 \cdot \bar{a}_y} U(\bar{r}'_{s1}) U(\bar{r}'_{s2}) \cdot \frac{e^{-jk_o r_{21} \sin\theta_z^i}}{(r_{21})^{1/2}} e^{jk_o(\bar{n}^f \cdot \bar{r}_{s2} - \bar{n}^i \cdot \bar{r}_{s1})} dx_{s1} dx_{s2} \tag{7a}$$

where,

$$r_{21} = |\bar{r}_{21}|, \quad \bar{n}_{21} = \bar{r}_{21}/r_{21} \tag{7b}$$

The above approximation is obviously valid only when $k_o r_{21} \gg 1$. However (7) can nevertheless be used to evaluate (6) since the scattering coefficients (D) vanish as $\bar{r}_{s2} \to \bar{r}_{s1}$. Note that the point 1 on the rough surface must be illuminated by the incident plane wave and visible at $\bar{r}_{s2}$ on the surface. Similarly point 2 must be illuminated by a point source at $\bar{r}'_{s1}$ and visible by the observer at $\bar{r}$ (see fig.1).

STATIONARY PHASE GEOMETRIC OPTICS APPROXIMATION

At very high frequencies the major contributions to the double scattered fields come only from the points 1 and 2 on the surface at which the phase

$$k_o \Phi(x_{s1}, x_{s2}) = k_o\, (\bar{n}^f \cdot \bar{r}_{s2} - \bar{n}^i \cdot \bar{r}_{s1} - r_{21} \sin\theta_z^i) \tag{8}$$

in the integrand of (7) is stationary. These stationary phase points are computed by differentiating the phase with respect to x_{s1} and x_{s2} respectively and solving the two equations simultaneously. When the stationary phase paths are isolated, (the distance between two paths is large compared to the wavelength), the geometrical optics approximation for isolated saddle points [1], [3] is used and compared with the results obtained by numerical integration (7). If the two stationary phase paths are close to each other (this occurs when the maximum slope of the rough surface is close to 45°) the geometrical optics expression [4] for nearby saddle points is used, (see fig.2). It is given as follows in terms of the Airy function :

$$G_d^f = \left(\frac{k_o}{2\pi}\right) \frac{e^{-jk_o r} e^{j\pi/2}}{(\rho)^{1/2} \sin\theta_z^i} e^{jk_o F} (2\pi)\, k_o^{-5/6} \left\{ \zeta_o^{1/4} \nu(\zeta) \left(\frac{f(x^1)\, e^{j\pi/4\delta_1}}{\sqrt{|D_1|}} + \frac{f(x^2)\, e^{j\pi/4\delta_2}}{\sqrt{|D_2|}} \right) + jk_o^{-1/3} \zeta_o^{-1/4} \nu'(\zeta) \left(\frac{f(x^1)\, e^{j\pi/4\delta_1}}{\sqrt{|D_1|}} - \frac{f(x^2)\, e^{j\pi/4\delta_2}}{\sqrt{|D_2|}} \right) \right\} \tag{9a}$$

where,

$$F = \frac{1}{2} [\, \Phi(x^1) + \Phi(x^2)\,] \tag{9b}$$

$$\zeta_o = \left(\frac{3}{4}\right)^{2/3} [\, \Phi(x^1) - \Phi(x^2)\,]^{2/3} \tag{9c}$$

$$\zeta = -\, k_o^{2/3}\, \zeta_o \tag{9d}$$

$$D_i = \left[\frac{\partial^2 \Phi(x_{s1}, x_{s2})}{\partial x_{s1}^2} \frac{\partial^2 \Phi(x_{s1}, x_{s2})}{\partial x_{s2}^2} - \frac{\partial^2 \Phi(x_{s1}, x_{s2})}{\partial x_{s1}\, \partial x_{s2}} \cdot \frac{\partial^2 \Phi(x_{s1}, x_{s2})}{\partial x_{s2}\, \partial x_{s1}} \right]_{x_{s1} = x_{s1i},\ x_{s2} = x_{s2i}}, \quad i = 1, 2 \tag{9e}$$

$$x^i = (x_{s1i}, x_{s2i}), \qquad i = 1, 2 \tag{9f}$$

$$\delta_i = \mathrm{sign}(D_i), \quad i = 1, 2 \tag{9g}$$

$$f(x^i) = \left[\frac{D(\bar{n}^f, \bar{n}_{21})}{\bar{n}_2 \cdot \bar{a}_y} \frac{D(\bar{n}_{21}, \bar{n}^i)}{\bar{n}_1 \cdot \bar{a}_y} \cdot \frac{U(\bar{r}'_{s1}) \cdot U(\bar{r}'_{s2})}{(r_{21})^{1/2}} \right]_{x_{s1} = x_{s1i},\ x_{s2} = x_{s2i}}, \quad i = 1, 2 \tag{9h}$$

In (9a) $\nu(\zeta)$ is defined by :

$$\nu(\zeta) = \sqrt{\pi}\, \mathrm{Ai}(\zeta) = \frac{1}{2\sqrt{\pi}} \int_{-\infty}^{\infty} e^{-j\left(\zeta x + \frac{x^3}{3}\right)} dx \tag{9i}$$

where $\mathrm{Ai}(\zeta)$ is the Airy function [7]. The argument of ζ in (9c) is chosen to be $\pi/3$ [5]. In this work the geometrical optics approximation is only used for backscatter at normal incidence, ($\sin\theta_z^i = 1$ in (3c)). Since there are two pairs of nearby stationary phase paths, we should apply (9) to each pair. If the maximum slope of the rough surface is less than 45° there are no stationary phase points on the surface and the above approximations cannot be used. The interference between the different doubly scattered contributions (see fig.2) could explain the observed fluctuations in the total scattered field near backscatter for normally incident excitations [6].

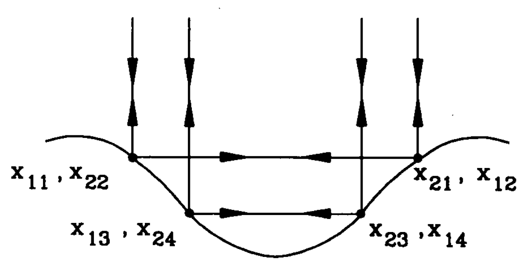

Fig. 2 Stationary phase paths for N=4

ILLUSTRATIVE EXAMPLES

For the one dimensional rough surface $h(x) = h_o \cos(2\pi x/\Lambda)$, several values of h_o and Λ are used to stimulate realizations of rough surfaces with different mean square heights and slopes. In figs.3-5 the like polarized scattered fields (single, double, and the total phasor sum double+single) are plotted in the incident plane ($\phi^f=0, \pi$) as functions of $\theta^f \cos\phi^f$ for different incident angles and different conductivities. In figs.3,4 the results show that for normal incidence the magnitude of the vertically and the horizontally polarized doubly scattered fields, $|E^{VV}|$ and $|E^{HH}|$ respectively, are most significant at normal scatter angles. In fig.3 ϵ_r= -11.43 - j1.24 for gold at λ_o=0.633 μm, and in fig.4 the surface is perfectly conducting. The mean square slopes are $<h_x^2>=0.5384$ in fig.3 and $<h_x^2>= 3.7$ in fig.4. In fig.5 the horizontally polarized scattered fields $|E^{HH}|$ are plotted in the plane of incidence ($\phi^f=0,\pi$) as functions of $\theta^f \cos\phi^f$. The excitation is a horizontally polarized plane wave incident at angle $\theta^i=65°$. The surface is perfectly conducting with mean square slope $<h_x^2>=2.1537$. The results show that for oblique incidence the observed enhanced backscatter is primarily due to single scatter. In fig.6 the cross polarized singly and doubly scattered fields $|E^{VH}|$ are plotted as functions of ϕ^f for $\sin\theta^f \sin\phi^f = \sin\theta^i \sin\phi^i$. Even though the surface h(x) is not a function of z depolarization occurs in this case because $\bar{n}^i$, $\bar{n}^f$, and $\bar{n}$ (local normal to the rough surface) are not in the same plane. The depolarized scattered fields vanish at $\phi^f=90°$ since for $\phi^i=90°$, $\theta^f=\theta^i$, and the integrands in (2) and (5) are antisymmetric over the sinusoidal surface h(x) [2].

A serial run of the computer program for the three dimensional integral (6) (on the supercomputer IBM/3090 at Cornell) takes about 1000 cpu seconds for $\theta^f=\theta^i=0$ to execute. It only takes 100 cpu seconds to evaluate the two dimensional integral (7) for $\theta^f=\theta^i=0$. The algorithm has been parallelized to reduce the wall clock time. This algorithm is considered coarse-grained. The integration subroutines called from the IMSL or the NAG libraries are considered the hot spots on the algorithm. For this reason subroutine level parallelism has been used (parallel tasks). The allocation of variables either to the shared memory or to the private memory was a major factor in the parallelization of this algorithm. The program to compute the vertically polarized double scattered fields at different angles of scatter was run in parallel with different numbers of processors. Comparisons of the corresponding wall-clock time and the cpu time are shown in Table 1. In this table the speed up is defined as follows

$$\text{speed-up} = \frac{\text{wall-clock time in serial}}{\text{wall-clock time in parallel}}$$

Table (1) indicates a significant reduction in the wall-clock time as a result of the parallelization of the program. Note that the last case in Table 1* had been run in batch and the machine was upgraded just at that time.

CONCLUDING REMARKS

The full-wave expressions for the single and the double scattered fields show that the double scatter contributes significantly to enhanced backscatter only for near normal incidence and when the mean square slope of the highly conductive surface is large. Moreover, when the maximum slope of the surface is larger than 45°, interference between the contributions from the different stationary phase paths (fig.2) result in the observed fluctuations of the enhanced doubly scattered fields (figs.3,4). This work provides physical insight to problems of scattering from random rough surfaces.

ACKNOWLEDGMENT

The computational work was conducted at the Cornell National Supercomputer Facility supported by NSF. The research is sponsored by the U.S. Army Research Office Contract DAAL0387-K-0085 and ONR Contract A00014-87-K-0177.

Table 1

WALL-CLOCK AND CPU TIMES FOR SERIAL AND PARALLEL PROCESSING

#angles (scatter)	Mode	wall-clock (seconds)	CPU (seconds)	#processors	speed-up
4	serial (interactive)	397	361	1	
4	parallel (interactive)	245	424	3+1	1.6
6	serial (interactive)	681	520	1	
6	parallel (interactive)	358	602	4+1	1.9
31	serial (batch)	3620	1717	1	
31	parallel (batch)	423	1530	4+1	8.5*

REFERENCES

[1] E. Bahar and M. El-Shenawee, "Full Wave Multiple Scattering From Rough Surfaces", presented at the IEEE International Symposium, Dallas, Texas, May 7-11, 1990.

[2] E. Bahar, "Full-Wave Solutions for the Depolarization of the Scattered Radiation Fields by Rough Surfaces of Arbitrary Slope", IEEE Trans. Antennas and Propagation, vol. AP-29, No. 3, pp. 443-454, May 1981.

[3] Born and Wolf, Principles of Optics, Pergaman Press, pp. 754, 1965.

[4] M.V. Fedoryuk, "The Stationary Phase Method Close Saddle Points in the Multi-dimensional Case", zh. vych. mat.4, no.4, pp. 671, 1964.

[5] N. Bleistein and R. Handelsman, Asymptotic Expansions of Integrals, Dover Publications, Inc., New York, ch. 9, pp. 371, 1986.

[6] K.A. O'Donnell and E.R. Mendez, "An experimental Study of Scattering from Characterized Random Surfaces", Optics Section, Blacket Laboratory, Imperial College, London SW7 2BZ, 1987.

[7] M. Abramowitz and I.A. Stegun, Handbook of Mathematical Functions, Applied Math Series 55, U.S. Dept. of Commerce, ch. 10.4, pp. 446, 1964.

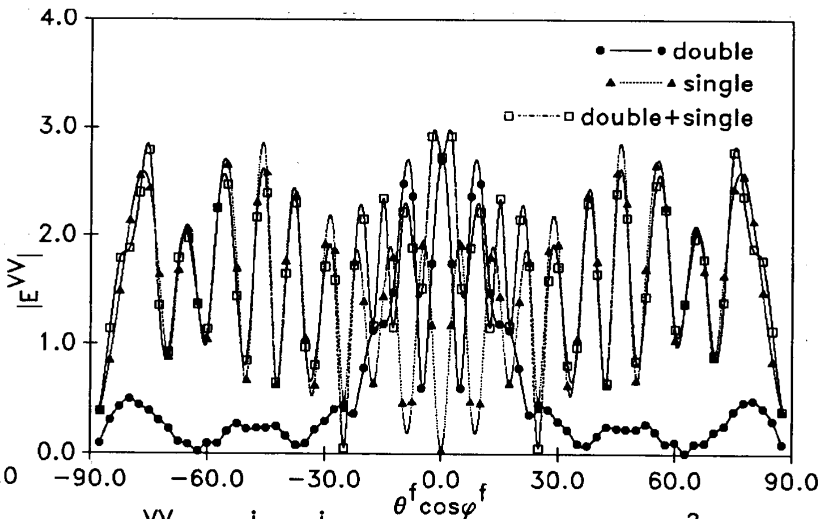

Fig.3 $|E^{VV}|$ for $\theta^i=0,\varphi^i=0,\Lambda=13.2793,h_o=2.1932,\langle h_x^2\rangle=0.5384$, max. slope=46.06°, $\epsilon_r=-11.43-j1.24$(gold), $\lambda_o=0.633\mu m,\mu_r=1$.

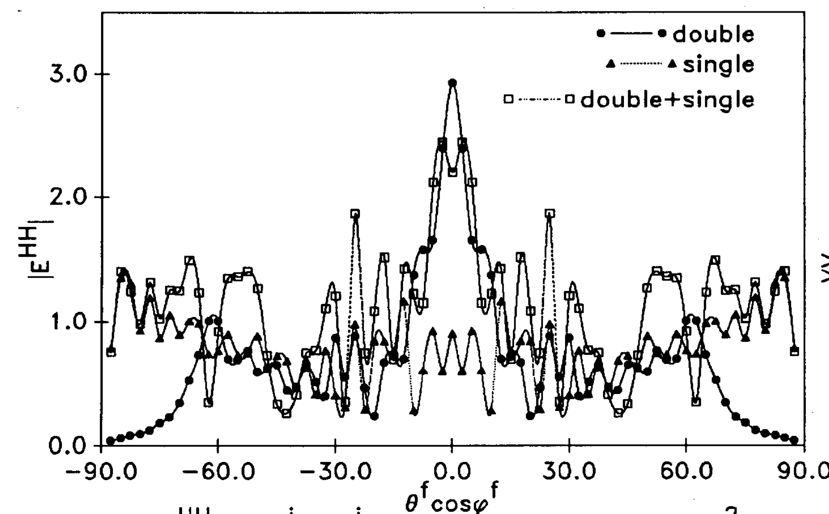

Fig.4 $|E^{HH}|$ for $\theta^i=0,\varphi^i=0,\Lambda=13.2793,h_o=5.7492,\langle h_x^2\rangle=3.7$, max. slope=69.81°, $|\epsilon_r|\gg1$(perfect conductor), $\mu_r=1$.

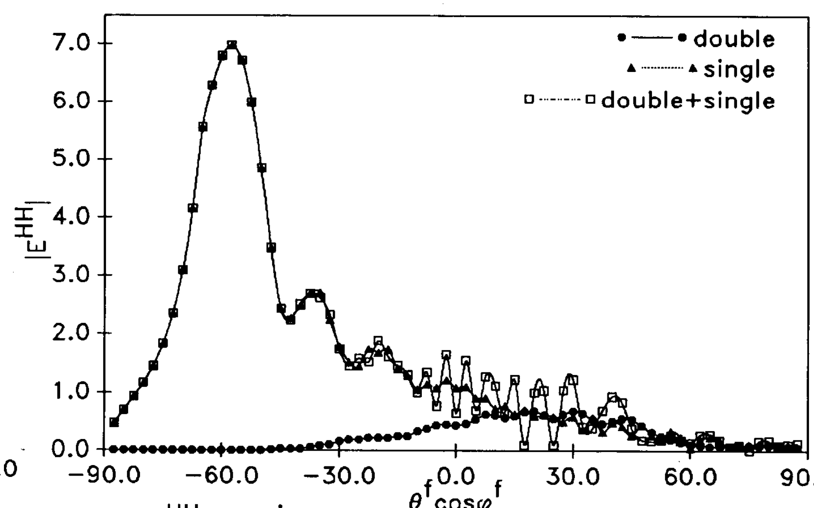

Fig.5 $|E^{HH}|$ for $\theta^i=65°,\varphi^i=0,\Lambda=12.1095,h_o=4.0,\langle h_x^2\rangle=2.1537$, max. slope=64.27°, $|\epsilon_r|\gg1$(perfect conductor), $\mu_r=1$.

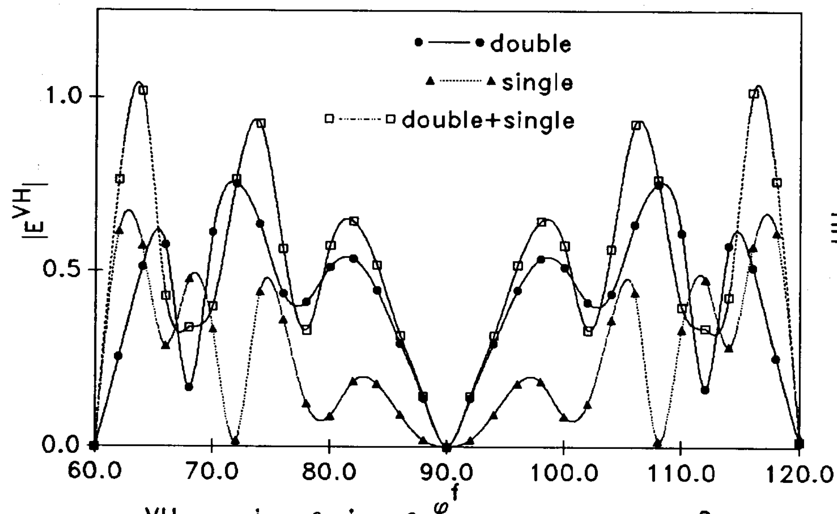

Fig.6 $|E^{VH}|$ for $\theta^i=60°,\varphi^i=90°,\Lambda=12.1095,h_o=4.0,\langle h_x^2\rangle=2.1537$, max. slope=64.27°, $\epsilon_r=-11.43-j1.24$(gold), $\lambda_o=0.633\mu m,\mu_r=1$.